

Article

Planar D- π -A Configured Dimethoxy Vinylbenzene Based Small Organic Molecule for Solution-Processed Bulk Heterojunction Organic Solar Cells

Shabaz Alam ¹, M. Shaheer Akhtar ², Abdullah ^{1,3}, Eun-Bi Kim ¹, Hyung-Shik Shin ^{1,4,*}
and Sadia Ameen ^{3,*}

¹ Energy Materials & Surface Science Laboratory, Solar Energy Research Center, School of Chemical Engineering, Jeonbuk National University, Jeonju 54896, Korea; shabaz@jbnu.ac.kr (S.A.); abdullahazmi@jbnu.ac.kr (A.); keb821@naver.com (E.-B.K.)

² New & Renewable Energy Material Development Center (NewREC), Jeonbuk National University, Buan-gun 56332, Korea; shaheerakhtar@jbnu.ac.kr

³ Advanced Materials & Devices Laboratory, Department of Bio-Convergence Science, Jeongeup Campus, Jeonbuk National University, Jeongeup 56212, Korea

⁴ Korea Basic Science Institute (KBSI), 169-148 Gwahak-ro, Yuseong-gu, Daejeon 34133, Korea

* Correspondence: hsshin@jbnu.ac.kr (H.-S.S.); sadiaameen@jbnu.ac.kr (S.A.)

Received: 29 July 2020; Accepted: 12 August 2020; Published: 19 August 2020



Abstract: A new and effective planar D- π -A configured small organic molecule (SOM) of 2-5-(3,5-dimethoxystyryl)thiophen-2-yl)methylene)-1H-indene-1,3(2H)-dione, abbreviated as DVB-T-ID, was synthesized using 1,3-indanedione acceptor and dimethoxy vinylbenzene donor units, connected through a thiophene π -spacer. The presence of a dimethoxy vinylbenzene unit and π -spacer in DVB-T-ID significantly improved the absorption behavior by displaying maximum absorbance at \sim 515 nm, and the reasonable band gap was estimated as \sim 2.06 eV. The electronic properties revealed that DVB-T-ID SOMs exhibited promising HOMO (-5.32 eV) and LUMO (-3.26 eV). The synthesized DVB-T-ID SOM was utilized as donor material for fabricating solution-processed bulk heterojunction organic solar cells (BHJ-OSCs) and showed a reasonable power conversion efficiency (PCE) of \sim 3.1% with DVB-T-ID:PC₆₁BM (1:2, *w/w*) active layer. The outcome of this work clearly reflects that synthesized DVB-T-ID based on 1,3-indanedione units is a promising absorber (donor) material for BHJ-OSCs.

Keywords: planar organic molecule; indanedione; dimethoxy vinylbenzene; organic solar cells; energy conversion

1. Introduction

In light of searching for renewable energy resources, solar energy is one of the most promising sustainable energy sources to fulfil global energy demand [1–5]. In the last few years, promising solar cells named solution-processed bulk heterojunction organic solar cells (BHJ-OSCs) have allured extensive research interest, owing to their marvelous advantages, such as their high power conversion efficiency (PCE) over conventional solar cells [6]. Recently, small organic molecules (SOMs) substituting strong electron donor (D) and acceptor (A) groups have been largely employed in BHJ-OSCs. Progressively, SOMs with a variety of D-A molecular networks are witnessed for the incessant upgradation of PCEs, rising from 1% to over 14% within two decades [7]. In BHJ-OSCs, the bulk phases considerably reduce the photoexcitation distance to generate a large amount of charges at separating interfaces, and also enhance the charge dissociation probability at the donor–acceptor interface [8,9]. SOMs and organic chromophores have shown fabulous semiconducting natures in

many optoelectronic devices due to their distinctive features, such as their flexibility, light weight, low temperature processing and potentially low cost over conventional silicon solar cells [10–14]. The photophysical and electrochemical properties of SOMs are highly tunable by designing and configuring chemical molecular structures [15]. One can assume that the appropriate selection of D-A moieties in SOMs can significantly enhance the charge mobility and contribute a large interfacial area for charge separation and collection [16].

Appreciable attention has recently been focused on exploring new small organic materials for the optimization of PCE and understanding the fundamental mechanism with the structure–property–performance relationship. Generally, low band gap SOMs with increased short circuit currents (J_{sc}) and minimum voltage loss are considered as deciding factors to maximizing photovoltaic (PV) performance [17]. The donor materials with deep HOMO levels (low ionization potential) are possible choices for obtaining a greater open circuit voltage (V_{oc}) without sacrificing J_{sc} in BHJ-OSCs [18]. To boost the absorption and electronic properties of SOMs, π electron systems in D-A or A-D-A based SOMs are helpful for accelerating charge mobility and rectifying the light absorption from the visible region to the NIR region [19]. The presence of a π bond system or π -spacers pushes more to break exciton or free charge carriers upon light absorption in an active layer [20]. SOMs based on π -conjugated electron systems have recently gained attention, owing to their high electron affinity and low ionization potentials, which define their donors and acceptors, respectively. The push–pull effect in donor–acceptor with π -conjugation arrangements can enable a fast intramolecular and photoinduced charge transfer, extend absorption in the visible region and ambipolar charge transport properties with high, balanced mobility can be observed in π -conjugated D- π -A systems [21–24]. In our previous report, Lamiaa et al. inserted an ethylene system as a π -spacer in D-A-D type SOMs and demonstrated a PCE of about 3.53%, with an improved fill factor (FF) = \sim 0.58, J_{sc} = \sim 8.71 mA/cm² and \sim V_{oc} of 0.698 V [25]. Abdullah et al. reported the synthesis of D- π -D type SOMs in which fluorene units behaved as π -spacers and displayed a reasonable PCE of \sim 2.13% [26]. The donor materials exhibited the deep HOMO levels for matching the energy level offset of PC₆₁BM acceptor. Additionally, thiophene units as π -linkers in SOMs also played a vital role in gaining excellent optoelectronic properties [27]. In this report, D- π -A SOM 25-(3,5-dimethoxystyryl) thiophen-2-yl) methylene)-1H-indene-1,3(2H)-dione, named as DVB-T-ID, has been synthesized and utilized as donor material for BHJ-OSCs. 2,3-Dihydro-1H-indene-1,3-dione (ID) acts as a potent acceptor moiety in various SOMs due to its stronger polarity and increased dielectric constant, and it displays a large interaction with the dimethoxy vinylbenzene (DVB) donor template [28,29]. Herein, a thiophene unit is fitted as a π group between a donor and acceptor in chromophore to establish a planar shape with the D- π -A system. The fabricated BHJ-OSCs with DVB-T-ID:PC₆₁BM active layers have achieved a moderate efficiency of \sim 3.1%, with J_{sc} = \sim 10.63 mA/cm², V_{oc} = \sim 0.637 V and FF = \sim 0.48 under an illumination of 100 mW/cm² (AM 1.5G).

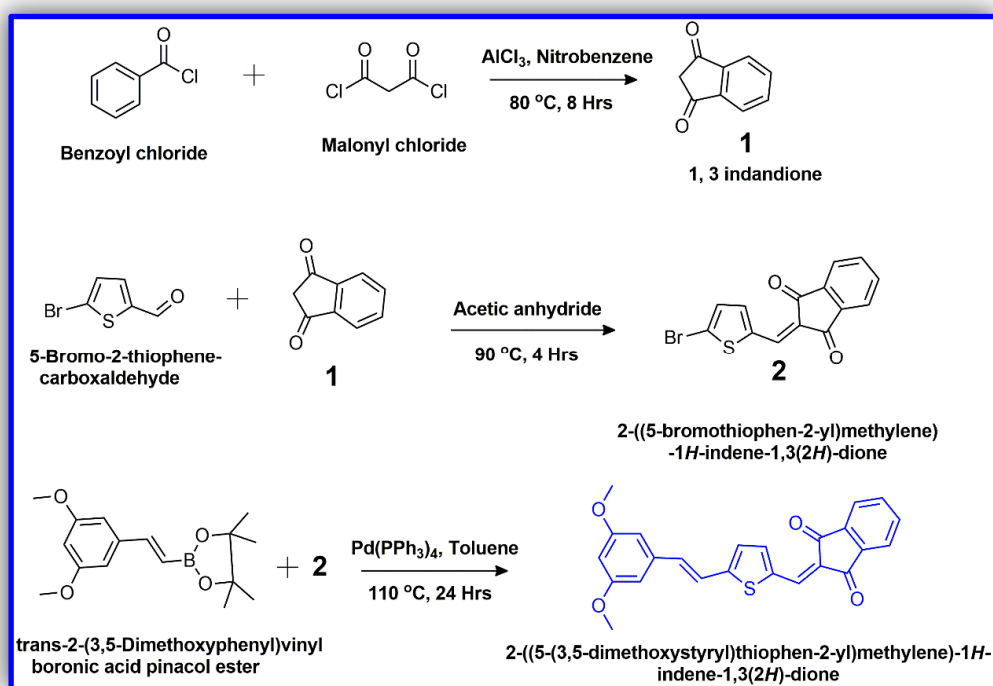
2. Materials and Methods

2.1. Materials and Equipment

All chemicals and reagents, including trans-2-(3,5-dimethoxyphenyl) vinylboronic acid pinacol ester, 5-bromo-2-thiophenecarboxaldehyde and tetrakis (triphenylphosphine) palladium (0) were procured from Sigma-Aldrich chemicals and employed without further purification.

2.2. Synthesis of DVB-T-ID

2-5-(3,5-dimethoxystyryl)thiophen-2-yl-methylene)-1H-indene-1,3(2H)-dione, (DVB-T-ID) organic chromophore was synthesized in several steps, as drawn in Scheme 1. Intermediates **1** and **2** were prepared as per the reported literature [13]. All the intermediates and DVB-T-ID were fully characterized by ¹HNMR, ¹³CNMR and mass spectrometry, and their plots are provided in the Supplementary Information (SI).



Scheme 1. The synthetic route for 2-((5-(3,5-Dimethoxystyryl) thiophen-2-yl)methylene)-1H-indene-1,3(2H)-dione (DVB-T-ID) chromophores.

2.3. Synthesis of 1, 3 Indandione (1)

Intermediate **1** was prepared in a similar fashion as reported in our previous work [13]. In a round bottom Schlenk flask, benzoyl chloride (0.913 g, 6.496 mmol), malonyl chloride (0.915 g, 6.496 mmol) and dry AlCl_3 (2.598 g, 19.490 mmol) were dissolved in anhydrous nitrobenzene (50 mL) and stirred at 80 °C for 8 h under argon atmosphere. After refluxing and cooling, the mixture was poured into an aqueous solution of Na_2CO_3 (120 mL). The organic layer was extracted with dichloromethane (4 × 50 mL), acidified with aqueous HCl (80 mL), separated by diethyl ether (2 × 80 mL) and later dried over Na_2SO_4 . Applying flash column chromatography, the organic crude product was purified using a mixture of diethyl ether:hexane (1:5, *v/v*) as eluent, followed by drying in a vacuum oven at 70 °C. The recrystallization of the obtained product was carried out in diethyl ether: EtOH (1:5, *v/v*) and finally collected as a pale yellow solid product (yield 67.09%, 0.637 g). ^1H NMR (500 MHz, CDCl_3 , ppm) δ : 7.94 (dd, $J = 2.6$ Hz, 2.3 Hz, 2H), 7.82 (dd, $J = 2.6$ Hz, 2.3 Hz, 2H), 3.23 (s, 2H). ^{13}C NMR (100 MHz, CDCl_3 , ppm) δ : 197.57, 143.40, 135.68, 123.27, 45.12. MS: m/z calc. for $[\text{C}_9\text{H}_6\text{O}_2 + \text{H}]^+$: 147.14. Found: 147.13.

2.4. Synthesis of 2-((5-Bromo-2-thiophen-2-yl) methylene)-1H-indene-1,3(2H)-dione (2)

In a round-bottom Schlenk tube, intermediate **1** (0.578 g, 3.95 mmol) and 5-bromo 2-thiophene-carboxaldehyde (1.132 g, 5.92 mmol) were mixed in acetic anhydride (30 mL) under Ar atmosphere for 30 min at 298 K. Then, the reaction temperature was elevated to 90 °C with stirring for 4 h [30] and cooled to room temperature, followed by an addition of plenty of water to the mixture to obtain precipitates. The subsequent precipitates were collected by filtration, dissolved in diethyl ether and dried over sodium sulfate (Na_2SO_4). The dried crystals were washed twice with ethyl acetate to obtain intermediate **2** as a spike-like yellow crystals (yield 66.07%, 0.835 g). ^1H NMR (500 MHz, CDCl_3 , ppm) δ : 7.94 (m, 2H), 7.89 (s, 1H), 7.76 (m, 2H), 7.61 (d, $J = 4.4$ Hz, 1H), 7.19 (d, $J = 4.2$ Hz, 1H). ^{13}C NMR (100 MHz, CDCl_3 , ppm) δ : 190.10, 189.67, 142.06, 141.93, 140.69, 138.90, 135.34, 135.27, 135.15, 131.50, 127.52, 124.74, 123.24, 123.17. MS: m/z calc. for $[\text{C}_{14}\text{H}_7\text{BrO}_2\text{S}]^+$: 319.17. Found: 319.62.

2.5. Synthesis of 2((5-(3,5-Dimethoxystyryl) thiophen-2-yl)methylene)-1H-indene-1,3(2H)-dione (DVB-T-ID)

Intermediate **2** (0.642 g, 2.01 mmol), trans-2-(3,5-dimethoxyphenyl) vinylboronic acid pinacol ester (0.875 g, 3.01 mmol), and a catalyst of 5 mol% Pd(PPh₃)₄ were mixed in anhydrous toluene (25 mL), followed by the addition of 5 mL of 2 M potassium carbonate (K₂CO₃), and refluxed at 110 °C for 24 h. After refluxing, the reaction mixture was poured into deionized (DI) water and washing with brine, DI. The extraction of the resultant organic part was done using a dichloromethane (DCM) solvent, followed by drying over MgSO₄. The washed organic phase was evaporated under reduced pressure using a rotary evaporator, and then further purified by a flash column using Diethyl ether–Hexane (1:3, *v/v*), dried in an oven and recrystallized twice with DCM–EtOH to obtain bright red crystals (yield 53.94%, 0.426g). ¹HNMR (500 MHz, (CD₃)₂SO, ppm) δ: 8.13 (d, J = 4.05 Hz, 1H), 7.96 (s, 1H), 7.88 (m, 4H), 7.56 (d, J = 16.2 Hz, 1H), 7.42 (d, J = 3.35 Hz, 1H), 7.24 (d, J = 16.2 Hz, 1H), 6.84 (d, J = 2.25 Hz, 2H), 6.42 (t, J = 2.25 Hz, 1H), 3.75 (s, 6H). ¹³CNMR (100 MHz, (CD₃)₂SO, ppm) δ: 189.93, 189.44, 161.25, 155.55, 145.58, 141.97, 140.38, 138.54, 136.33, 136.06, 136.02, 135.91, 133.49, 128.43, 123.92, 123.24, 123.06, 122.58, 105.59, 101.87, 55.86. MS: *m/z* calc. for [C₂₈H₂₄O₂S₃ + H]⁺: 403.46. Found: 403.60.

2.6. Device Fabrication

For the fabrication of BHJ-OSCs, ITO (12–16 Ω/sq, Samsung-electronics, Suwon, South Korea) glass substrates were cleaned by sonication with detergent, acetone, DI water and isopropyl alcohol for 10 min and dried in an oven. Firstly, a compact titanium dioxide (c-TiO₂) layer was deposited on the ITO substrate using a spin coater at ~3000 rpm for ~30 s, subsequently annealed at ~150 °C in a vacuum oven for 10 min and subjected to 450 °C in a furnace for 30 min. The blended solutions for the photoactive layers were prepared by mixing DVB-T-ID and PC₆₁BM in different weight percentages (DVB-T-ID:PC₆₁BM, 1:1, 1:2, and 1:3, *w/w*) in chlorobenzene and stirred at 60 °C for 1 h to obtain the solutions. Thereafter, these solutions were spin coated onto a c-TiO₂ layer with a scan rate of ~2000 rpm for ~40 s and quickly subjected to annealing in a vacuum oven at ~70 °C for 10 min. A top electrode of gold (Au, ~100 nm thickness) was deposited over the DVB-T-ID:PC₆₁BM/c-TiO₂/ITO by controlled thermal evaporation to complete the device configuration of Au/DVB-T-ID:PC₆₁BM/c-TiO₂/ITO for solution-processed BHJ-OSC.

2.7. Characterizations

FTIR spectroscopy was executed by an FTIR-4100 (JASCO, Tokyo, Japan) spectrometer to investigate the structural features of SOMs. An FT-NMR spectrophotometer (JEOL, Tokyo, Japan) was applied for the proton/¹³C nuclear magnetic resonance (¹HNMR (500 MHz) and ¹³CNMR (125 MHz)) spectra and measured the chemical shift (δ) in ppm, using tetramethylsilane (TMS) as an internal standard in the reference solvents of CDCl₃ and (CD₃)₂SO. A XEVO TQ-S spectrophotometer was used to determine the mass spectra (MS) of synthesized SOMs. The UV-Vis (V-670 (JASCO, Tokyo, Japan)) and photoluminescence (PL, FP-6500 fluorometer, excitation wavelength: 480 nm) spectroscopies were utilized for investigating the optical behavior of SOMs. Thermogravimetric analysis (TGA) and differential scanning calorimetry (DSC) were measured by a TA instrument (DSC-2910, Q-50) at the fixed scan rate of 10 °C/min under N₂ gas. The electrochemical cyclic voltammogram (CV) was evaluated by a WPG 100 Potentiostat/Galvanostat (WonaTech) with three electrode electrochemical systems, including a working SOM-coated glassy carbon electrode, saturated calomel reference electrode (SCE) and a counter electrode composed of platinum wire, using 0.1 M TBAPF₆ in acetonitrile as the supporting electrolyte at a scan rate of 150 mV/s. The surface morphologies of the blended thin films were analyzed by AFM in tapping and 3D mode, using an AFM Nanoscope instrument. To extract the photovoltaic parameters, the current density-voltage (J-V) characteristics of the solar cells were tested under 1 sun (AM 1.5 G, 100 mW/cm²) using the light source of a metal halide lamp (Phillips, 1000 W, Newyork City, NY, USA). The radiation power of the light was fixed by using a Si photodiode as a reference, calibrated at NREL (Golden, CO, USA).

3. Results and Discussion

3.1. Thermal Properties of DVB-T-ID SOM

The thermal behavior and stability of DVB-T-ID were investigated by measuring the TGA and DSC, as shown in Figure 1. The TGA plot displays a high decomposition temperature (T_d) at ~ 330 °C with 5% weight loss, indicating a high thermal stability of DVB-T-ID SOMs. In support, the DSC thermogram (Figure 1b) shows a sharp melting temperature (T_m) at ~ 188 °C and an exothermic crystalline transition (T_c) occurs at ~ 370 °C. Strong T_m and T_c peaks are attributed to a liquid crystal (LC) transition phase and a good intermolecular cohesion in D- π -A, generally due to self-organizational behavior in a solid state, resulting in π - π stacking and possible phase transition [31,32].

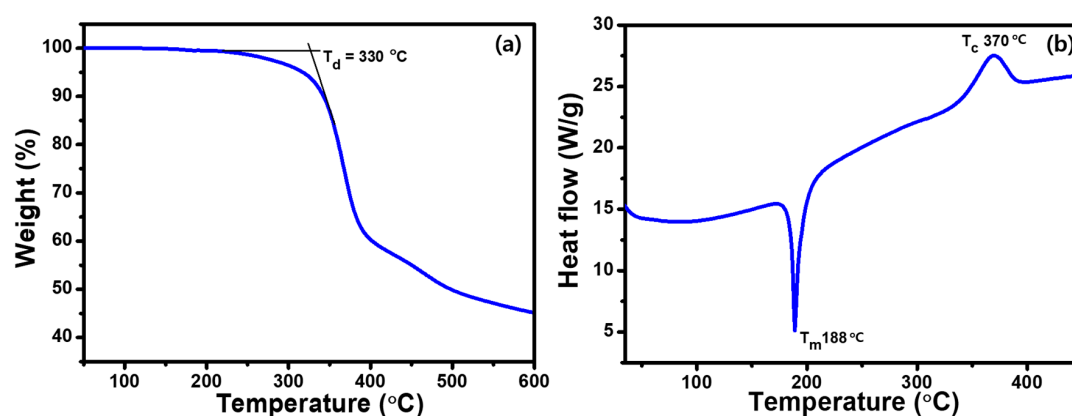


Figure 1. (a) Thermogravimetric analysis (TGA) and (b) differential scanning calorimetry (DSC) plots of DVB-T-ID SOMs.

3.2. Optical Properties of DVB-T-ID SOM

The solubility test reveals that the synthesized DVB-T-ID SOM presents excellent solubility in most common laboratory solvents like chlorobenzene, tetrahydrofuran (THF) and chloroform. UV-Vis spectroscopy has been performed to explain the absorption behavior of DVB-T-ID SOMs, as depicted in Figure 2a. In chloroform, the prominent absorption band, at ~ 483 nm, and weak absorption, at ~ 315 nm, are detected by DVB-T-ID, as summarized in Table 1. These absorption bands basically represent π - π^* (weak absorption) and n - π^* (strong absorption) transitions, which might be beneficial for the charge transfer process [33]. As compared to the solution sample, the significant red shift with the absorption band at ~ 515 nm is observed in the DVB-T-ID solid thin film, suggesting the presence of strong intramolecular interaction, backbone planarity and π - π stacking in a solid state [34,35]. Using the absorption onset value of the maximum absorption peak in Figure 2a, the optical energy band gap (E_g^{opt}) of the DVB-T-ID thin film is estimated as ~ 2.06 eV by considering an equation of $E_g^{opt} = 1240/\lambda_{onset}$. To understand the charge carriers and luminescence properties of the DVB-T-ID SOM, the PL spectroscopies (Figure 2b) are studied in a chloroform solution and in thin films. The DVB-T-ID SOM displays a strong emission peak at ~ 560 and ~ 620 nm in chloroform solution and thin film, respectively. The red shift in the thin film is related to the inter-chromophoric aggregation or planarization of organic molecules.

Table 1. Thermal, optical and electrochemical parameters of the synthesized DVB-T-ID OSM.

Chromophore	λ_{max}^a (nm)	λ_{max}^b (nm)	λ_{max}^c (nm)	λ_{max}^d (nm)	HOMO ^e (eV)	LUMO ^f (eV)	E_g^{opt} ^g (eV)
DVB-T-ID	483	515	560	602	5.32	3.26	2.06

^a Maximum absorbance value in chloroform solution. ^b Maximum absorbance value for SOM thin film. ^c PL emission peak in chloroform solution. ^d PL emission peak for SOM thin film. ^e Using the oxidation onset potential of the cyclic voltammogram. ^f LUMO = HOMO + E_g^{opt} . ^g Found using the following equation: $E_g^{opt} = 1240/\lambda_{edge}$.

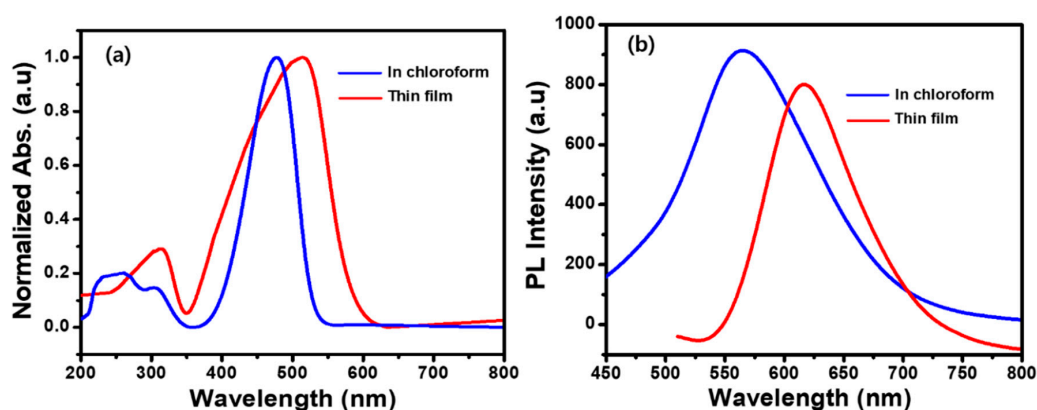


Figure 2. (a) UV-Vis absorption and (b) photoluminescence (PL) spectra of a DVB-T-ID SOM in a chloroform solvent and solid state thin film.

The donor–acceptor (DVB-T-ID:PC₆₁BM) thin film was further characterized by UV-Vis absorption spectra to investigate the outcome of photon harvesting. Figure 3a depicts the UV-Vis spectra of DVB-T-ID:PC₆₁BM thin films with different blend ratios of 1:1, 1:2 and 1:3, *w/w*. All blended thin films exhibit a broad absorption which covers the visible region of ~400 to ~600 nm, suggesting DVB-T-ID as a competent light-harvesting OSM for BHJ-OSCs. The DVB-T-ID:PC₆₁BM (1:2, *w/w*) thin film displays the highest absorption intensity, which might be associated with the non-aggregated, uniform and smooth surface of the thin film. Furthermore, the PL spectra of DVB-T-ID:PC₆₁BM blend thin films are measured to investigate the charge transfer behavior from donor to acceptor, as shown in Figure 3b. As compared with the intensity of PL emission in the DVB-T-ID thin film, a strong quenching occurs in the DVB-T-ID:PC₆₁BM blend thin films, confirming a good exciton dissociation and a fast charge transfer at the interface of DVB-T-ID:PC₆₁BM [36]. The improved charge transportation in the DVB-T-ID:PC₆₁BM blend thin film might impart to generate a high photocurrent. Hence, DVB-T-ID:PC₆₁BM blend thin films are promising for fabricating efficient BHJ-OSCs.

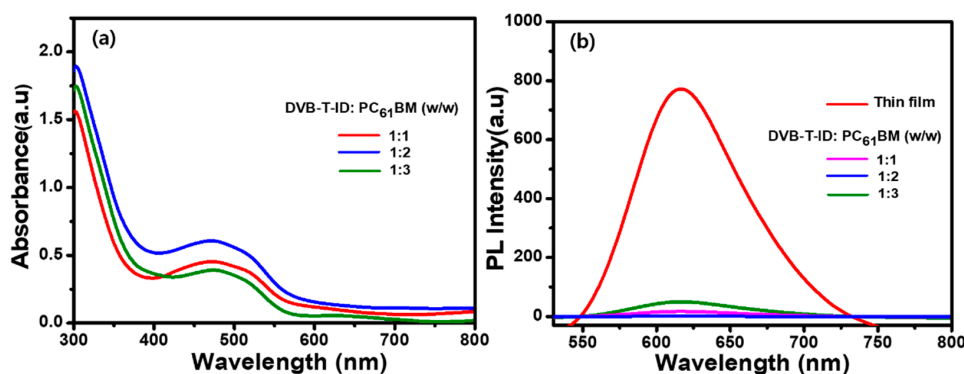


Figure 3. (a) UV-Vis absorption and (b) PL spectra of DVB-T-ID:PC₆₁BM thin films of different blend ratios (1:1, 1:2, and 1:3 (*w/w*)).

3.3. Electrochemical and Photovoltaic Properties of DVB-T-ID OSM

The electronic properties, in terms of HOMO and LUMO energy levels, were studied by performing cyclic voltammetry (CV) of a DVB-T-ID thin film in freshly prepared 0.1 M TBAPF₆ in acetonitrile at a scan rate of 150 mV/s, using Fc/Fc⁺ as an external reference. From Figure 4, the DVB-T-ID thin film records an oxidation onset potential value of +0.30 V. For the calculation of HOMO and LUMO energy levels, the following equations are employed [13]:

$$\text{HOMO} = -e [E_{\text{ox}} - E_{1/2} (\text{Fc}/\text{Fc}^+) + 4.8] \text{ eV}$$

$$\text{LUMO} = (\text{HOMO} + E_g^{\text{opt}}) \text{ eV}$$

where E_{ox} and $E_{1/2}$ are the onset oxidation potential of the donor material and the redox potential of Fc/Fc^+ versus Ag/AgCl , respectively. Using the above equations, the DVB-T-ID SOM possesses an impressive HOMO of ~ -5.32 eV and LUMO of ~ -3.26 eV. The energy offset between the LUMO and HOMO of the donor DVB-T-ID SOM with a PC_{61}BM acceptor is sufficiently high and provides enough of a driving force for charge dissociation.

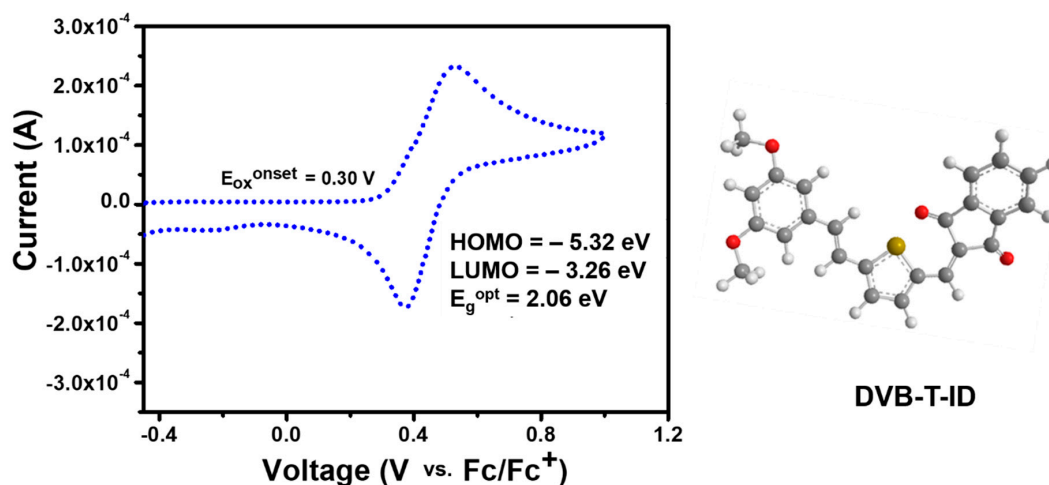


Figure 4. Cyclic voltammetry and molecular structure of a DVB-T-ID thin film in 0.1 M TBAPF₆ as the supporting electrolyte in an anhydrous acetonitrile solution, with ferrocene as an external reference.

Figure 5a illustrates the band energy levels diagram of BHJ-OSCs fabricated with a DVB-T-ID:PC₆₁BM active layer. As seen in the electrochemical and optical studies, the newly designed D- π -A (DVB-T-ID) displays a good optical bandgap and molecular energy levels, which originate from the introduction of a π -spacer in the DVB and ID units. It is seen that the HOMO value of DVB-T-ID SOMs is fairly suitable to the HOMO level (-6.45 eV) of PC₆₁BM. The LUMO counterpart of the donor and the HOMO counterpart of the acceptor are rather large for exciton binding energy, which considerably eases the exciton dissociation at the interface of DVB-T-ID:PC₆₁BM. This alignment of HOMO and LUMO energy levels in DVB-T-ID:PC₆₁BM might increase the charge transfer at the interface of the donor-acceptor layer. To evaluate photovoltaic behavior, the synthesized DVB-T-ID OSM as a donor material was applied in fabricating the BHJ-OSCs. The photovoltaic performance of fabricated BHJ-OSCs with a DVB-T-ID:PC₆₁BM active layer was tested by measuring the J-V characteristics under light illumination at 100 mW/cm² (AM1.5). Figure 5b presents the J-V curves of fabricated BHJ-OSCs with different DVB-T-ID:PC₆₁BM blend ratios (1:1, 1:2, and 1:3 w/w). The BHJ-OSC with DVB-T-ID:PC₆₁BM (1:2, w/w) exhibits a PCE = $\sim 3.1\%$, a high J_{sc} = ~ 10.63 mA/cm², V_{oc} = ~ 0.637 V and a high FF = $\sim 0.48\%$. The obtained photovoltaic parameters are higher than the reported OSCs of similar structures, as shown in Table 2. The high J_{sc} of BHJ-OSCs is ascribed to the broad wavelength in the visible region and the good light scattering properties of the DVB-T-ID:PC₆₁BM thin film. Herein, a low V_{oc} value might attribute to a higher LUMO (~ -3.26 eV) value of the DVB-T-ID donor, as compared with the LUMO energy level of the PC₆₁BM (~ -4.37 eV). It is notable that the fabricated BHJ-OSC exhibits a relatively high FF, without the addition of additives or promoters in the active layer. Generally, the FF in organic solar cells (OSCs) relies on the surface properties of semiconducting materials, like charge mobility and the impact of morphology of the active layer [37,38]. Herein, a considerable advancement in the morphology of the active layer of DVB-T-ID:PC₆₁BM (1:2, w/w) at the nanoscale level delivers a high FF, as discussed in AFM studies.

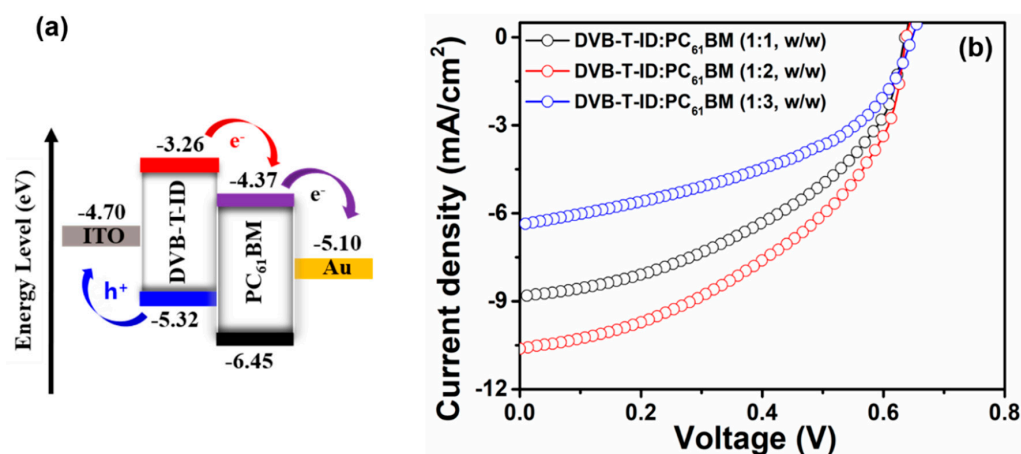


Figure 5. (a) Band structure of BHJ-OSC and (b) J-V curves of fabricated BHJ-OSCs with an active layer of DVB-T-ID:PC₆₁BM of blend ratios 1:1 and 1:2 (*w/w*).

To explore the morphological behavior of the blend films, AFM measurements of DVB-T-ID:PC₆₁BM thin films in tapping mode were performed. Figure 6 presents the AFM images of DVB-T-ID:PC₆₁BM thin films with different blend ratios. With a blend ratio of 1:2, *w/w*, the DVB-T-ID:PC₆₁BM thin film displays smooth and uniform morphology, exhibiting small grains at a nanoscale level, as shown in Figure 6c. In addition, the height and 3D images of the DVB-T-ID:PC₆₁BM (1:2, *w/w*) thin film again confirm the smooth surface, which might be a consequence of the well-mixed donor–acceptor in blend form, leading to favorable interpenetrating networks with an appropriate degree of phase separation and a high charge carrier extraction [39]. A low root-mean-square roughness (R_{rms}) value of ~4.37 nm was estimated for the DVB-T-ID:PC₆₁BM (1:2, *w/w*) thin film, whereas other blend ratios presented high R_{rms} values. The blend film roughness is basically controlled with the amount of the PC₆₁BM acceptor in the blend film. Herein, further increments of the PC₆₁BM acceptor (1:3, *w/w*) lead to the formation of large aggregates. Large aggregates in a DVB-T-ID:PC₆₁BM (1:3, *w/w*) thin film might prevent an immediate charge separation, which is also supported by PL quenching in (1:3, *w/w*) and thus results in poor photovoltaic performances. Moreover, a high FF of BHJ-OSCs might be due to good surface smoothness, uniform grain sizes and low surface roughness [40], which might result in a fast charge extraction. Therefore, the optimal active layer of DVB-T-ID:PC₆₁BM (1:2, *w/w*) evidences the good miscibility of DVB-T-ID and PC₆₁BM, which might be helpful in forming a bi-continuous network structure through quick phase segregation. This phenomenon promotes the proper charge carrier collection for BHJ solar cell devices, resulting in a high photocurrent and a high PCE.

Table 2. Summary of photovoltaic parameters of the fabricated and reported BHJ-OSCs.

Active Layer	V_{oc} (V)	J_{sc} (mA/cm ²)	FF	PCE (%)	Ref.
OIYM(4):PC ₆₁ BM	0.74	6.65	0.47	2.34	[41]
DDIN7T:PC ₆₁ BM	0.76	3.14	0.28	0.66	[42]
D2R(8+2)7T:PC ₆₁ BM	0.92	6.77	0.39	2.46	[43]
DTIDTQX:C ₇₀	0.71	6.24	0.38	1.70	[44]
DINCNDTS:PC ₇₁ BM	0.86	1.82	0.37	0.58	[45]
InTTD:PC ₆₁ BM	0.71	2.69	0.32	0.62	[30]
InCNTTD:PC ₆₁ BM	0.82	3.95	0.38	1.22	[30]
DVB-T-ID:PC ₆₁ BM (1:1, <i>w/w</i>)	0.634	8.85	0.46	2.57	This work
DVB-T-ID:PC ₆₁ BM (1:2, <i>w/w</i>)	0.637	10.63	0.48	3.10	This work
DVB-T-ID:PC ₆₁ BM (1:3, <i>w/w</i>)	0.647	6.39	0.45	1.86	This work

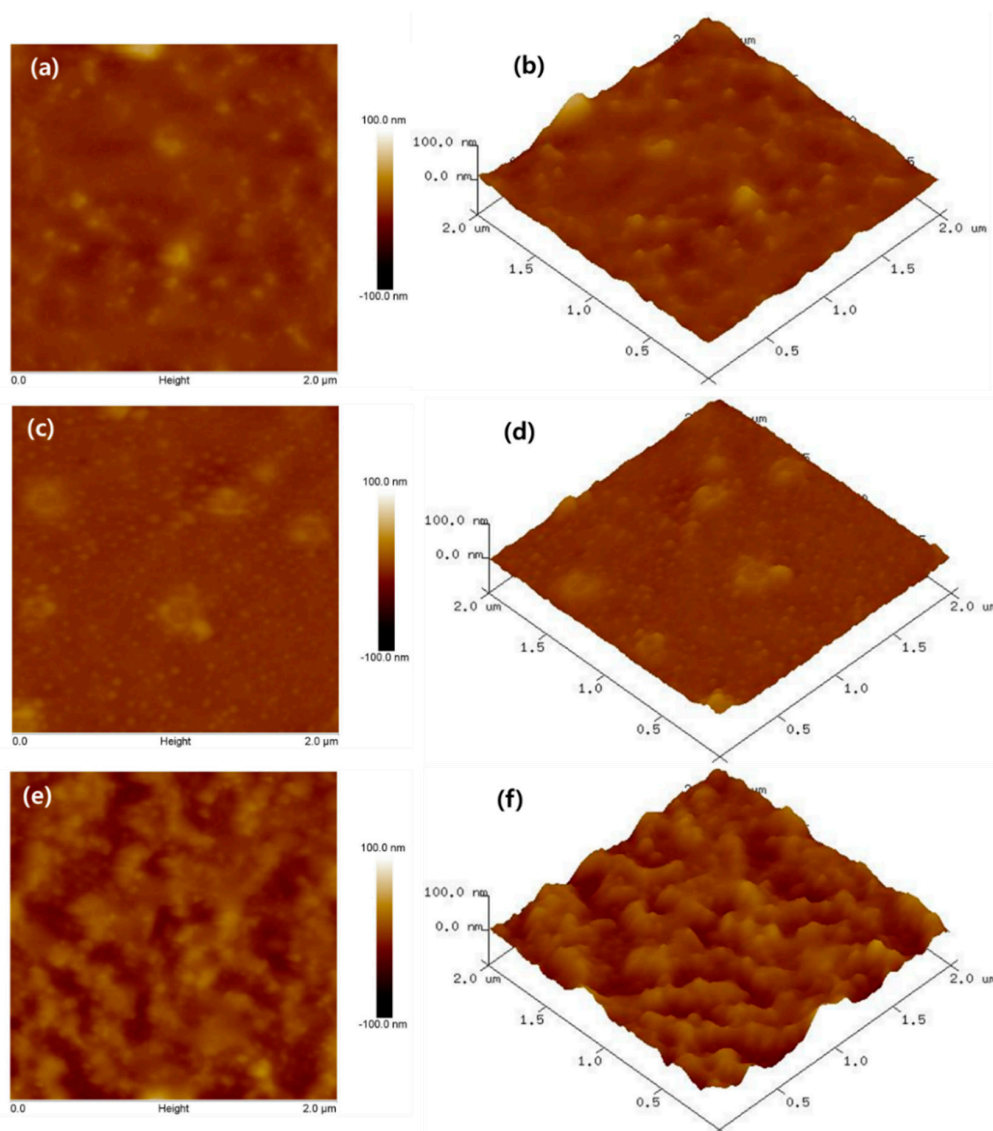


Figure 6. Representative AFM height and 3D images of (a,b) 1:1, w/w , (c,d) 1:2, w/w and (e,f) 1:3, w/w of DVB-T-ID:PC₆₁BM blend thin films.

4. Conclusions

New and effective planar D- π -A (DVB-T-ID) SOMs based on 1,3-indanedione acceptor and dimethoxy vinylbenzene donor units are synthesized and used as donor or absorber materials for BHJ-OSCs. DVB-T-ID SOMs show a good solubility in most of the common solvents and demonstrate promising photophysical properties. The moderate HOMO and LUMO energy levels of ~ 5.32 eV and ~ 3.26 eV were obtained for DVB-T-ID SOMs. As a donor material, BHJ-OSC fabricated with DVB-T-ID:PC₆₁BM (1:2, w/w) achieved a moderate PCE of $\sim 3.1\%$ and a J_{SC} of ~ 10.63 mA/cm², along with an FF of ~ 0.48 . In this work, the enhanced PCE and photocurrent density might be associated with good miscibility and intermolecular charge transfer between the DVB-T-ID and PC₆₁BM moieties.

Supplementary Materials: The following are available online at <http://www.mdpi.com/2076-3417/10/17/5743/s1>.

Author Contributions: Conceptualization, S.A. (Shabaz Alam) and M.S.A.; Data curation, A.; Formal analysis, A. and E.-B.K.; Funding acquisition, E.-B.K. and H.-S.S.; Investigation, S.A. (Shabaz Alam); Methodology, S.A. (Shabaz Alam); Project administration, S.A. (Sadia Ameen); Resources, S.A. (Sadia Ameen); Software, E.-B.K.; Supervision, H.-S.S.; Visualization, A.; Writing—review & editing, M.S.A., H.-S.S. and S.A. (Sadia Ameen). All authors have read and agreed to the published version of the manuscript.

Funding: This research received no external funding.

Acknowledgments: This work is fully supported by the National Research Foundation of Korea (NRF) grant funded by the Korea government (MSIT) (NRF2019R1F1A1063999). This research was also supported by the Korea Basic Institute under the R&D program (Project No. D010710) supervised by the Ministry of Science and ICT. This paper was supported by research funds for newly appointed professors of Jeonbuk National University in 2018.

Conflicts of Interest: The authors declare no conflict of interest.

References

1. Takacs, C.J.; Sun, Y.; Welch, G.C.; Pérez, L.A.; Liu, X.; Wen, W.; Bazan, G.C.; Heeger, A.J. Solar cell efficiency, self-assembly, and dipole–dipole interactions of isomorphous narrow-band-gap molecules. *J. Am. Chem. Soc.* **2012**, *134*, 16597–16606. [[CrossRef](#)]
2. Bernède, J.C. Organic photovoltaic cells: History, principle and techniques. *J. Chil. Chem. Soc.* **2008**, *53*, 1549–1564. [[CrossRef](#)]
3. Mazzi, K.A.; Luscombe, C.K. The future of organic photovoltaics. *Chem. Soc. Rev.* **2015**, *44*, 78–90. [[CrossRef](#)] [[PubMed](#)]
4. Bagher, A.M. Comparison of organic solar cells and inorganic solar cells. *Int. J. Renew. Sustain. Energy* **2014**, *3*, 53. [[CrossRef](#)]
5. Spanggaard, H.; Krebs, F.C. A brief history of the development of organic and polymeric photovoltaics. *Sol. Energy Mater. Sol. Cells* **2004**, *83*, 125–146. [[CrossRef](#)]
6. Ameen, S.; Rub, M.A.; Kosa, S.A.; Alamry, K.A.; Akhtar, M.S.; Shin, H.-S.; Seo, H.-K.; Asiri, A.M.; Nazeeruddin, M.K. Perovskite solar cells: Influence of hole transporting materials on power conversion efficiency. *ChemSusChem* **2016**, *9*, 10–27. [[CrossRef](#)] [[PubMed](#)]
7. Zhou, R.; Jiang, Z.; Yang, C.; Yu, J.; Feng, J.; Adil, M.A.; Deng, D.; Zou, W.; Zhang, J.; Lu, K.; et al. All-small-molecule organic solar cells with over 14% efficiency by optimizing hierarchical morphologies. *Nat. Commun.* **2019**, *10*, 1–9. [[CrossRef](#)] [[PubMed](#)]
8. Yao, H.-B.; Ge, J.; Mao, L.-B.; Yan, Y.-X.; Yu, S.-H. 25th anniversary article: Bulk heterojunction solar cells: Understanding the mechanism of operation. *Adv. Mater.* **2014**, *26*, 192. [[CrossRef](#)]
9. Bredas, J.-L.; Norton, J.E.; Cornil, J.; Coropceanu, V. Molecular understanding of organic solar cells: The challenges. *Acc. Chem. Res.* **2009**, *42*, 1691–1699. [[CrossRef](#)]
10. Liu, Q.; Jiang, Y.; Jin, K.; Qin, J.; Xu, J.; Li, W.; Xiong, J.; Liu, J.; Xiao, Z.; Sun, K.; et al. 18% efficiency organic solar cells. *Sci. Bull.* **2020**, *65*, 272–275. [[CrossRef](#)]
11. Ma, X.; Wang, J.; Gao, J.; Hu, Z.; Xu, C.; Zhang, X.; Zhang, F. Achieving 17.4% efficiency of ternary organic photovoltaics with two well-compatible nonfullerene acceptors for minimizing energy loss. *Adv. Energy Mater.* **2020**, 2001404. [[CrossRef](#)]
12. Vandewal, K.; Benduhn, J.; Nikolis, V.C. How to determine optical gaps and voltage losses in organic photovoltaic materials. *Sustain. Energy Fuels* **2018**, *2*, 538–544. [[CrossRef](#)]
13. Alam, S.; Akhtar, M.S.; Abdullah, Kim, E.-B.; Shin, H.-S.; Ameen, S. New energetic indandione based planar donor for stable and efficient organic solar cells. *Sol. Energy* **2020**, *201*, 649–657. [[CrossRef](#)]
14. Yeboah, D.; Singh, J. Study of the Contributions of donor and acceptor photoexcitations to open circuit voltage in bulk heterojunction organic solar cells. *Electronics* **2017**, *6*, 75. [[CrossRef](#)]
15. Van Der Poll, T.S.; Love, J.A.; Nguyen, T.; Bazan, G.C. Non-basic high-performance molecules for solution-processed organic solar cells. *Adv. Mater.* **2012**, *24*, 3646–3649. [[CrossRef](#)] [[PubMed](#)]
16. Gautam, P.; Misra, R.; Siddiqui, S.A.; Sharma, G.D. Unsymmetrical donor–acceptor–acceptor– π –donor type benzothiadiazole-based small molecule for a solution processed bulk heterojunction organic solar cell. *ACS Appl. Mater. Interfaces* **2015**, *7*, 10283–10292. [[CrossRef](#)] [[PubMed](#)]
17. Nazim, M.; Ameen, S.; Akhtar, M.S.; Seo, H.-K.; Shin, H.-S. Furan-bridged thiazolo [5,4-d] thiazole based D- π -A- π -D type linear chromophore for solution-processed bulk-heterojunction organic solar cell. *RSC Adv.* **2015**, *5*, 6286–6293. [[CrossRef](#)]
18. Bäessler, H.; Kohler, A.-L. Charge transport in organic semiconductors. *Top. Curr. Chem.* **2012**, *312*, 1–65.

19. Zhou, T.; Jia, T.; Kang, B.; Li, F.; Fahlman, M.; Wang, Y. Nitrile-substituted QA derivatives: New acceptor materials for solution-processable organic bulk heterojunction solar cells. *Adv. Energy Mater.* **2011**, *1*, 431–439. [[CrossRef](#)]
20. Yao, H.; Ye, L.; Zhang, H.; Li, S.; Zhang, S.; Hou, J. Molecular design of benzodithiophene-based organic photovoltaic materials. *Chem. Rev.* **2016**, *116*, 7397–7457. [[CrossRef](#)]
21. Wagner, K.; Crowe, L.L.; Wagner, P.; Gambhir, S.; Partridge, A.C.; Earles, J.C.; Clarke, T.M.; Gordon, K.C.; Officer, D.L. Indanedione-substituted poly (terthiophene)s: Processable conducting polymers with intramolecular charge transfer interactions. *Macromolecules* **2010**, *43*, 3817–3827. [[CrossRef](#)]
22. Zhu, L.; Yi, Y.; Wei, Z. Exciton binding energies of nonfullerene small molecule acceptors: Implication for exciton dissociation driving forces in organic solar cells. *J. Phys. Chem. C* **2018**, *122*, 22309–22316. [[CrossRef](#)]
23. Menke, S.M.; Holmes, R.J. Exciton diffusion in organic photovoltaic cells. *Energy Environ. Sci.* **2014**, *7*, 499–512. [[CrossRef](#)]
24. Mikhnenko, O.V.; Blom, P.W.M.; Nguyen, T.-Q. Exciton diffusion in organic semiconductors. *Energy Environ. Sci.* **2015**, *8*, 1867–1888. [[CrossRef](#)]
25. Fijahi, L.; Akhtar, M.S.; Abdullah; Kim, E.-B.; Seo, H.-K.; Shin, H.S.; Ameen, S. Investigation of newly designed asymmetric chromophore in view of power conversion efficiency improvements for organic solar cells. *Mater. Lett.* **2020**, *260*, 126865. [[CrossRef](#)]
26. Abdullah; Ameen, S.; Akhtar, M.S.; Fijahi, L.; Kim, E.-B.; Shin, H.S. Solution processed bulk heterojunction organic solar cells using small organic semiconducting materials based on fluorene core unit. *Opt. Mater.* **2019**, *91*, 425–432. [[CrossRef](#)]
27. Nazim, M.; Abdullah; Akhtar, M.S.; Kim, E.-B.; Shin, H.-S.; Ameen, S. Underlying effects of diiodooctane as additive on the performance of bulk heterojunction organic solar cells based small organic molecule of isatin-core moiety. *Synth. Met.* **2020**, *261*, 116304. [[CrossRef](#)]
28. Deng, D.; Zhang, Y.; Zhang, J.; Wang, Z.; Zhu, L.; Fang, J.; Xia, B.; Wang, Z.; Lu, K.; Ma, W.; et al. Fluorination-enabled optimal morphology leads to over 11% efficiency for inverted small-molecule organic solar cells. *Nat. Commun.* **2016**, *7*, 13740. [[CrossRef](#)]
29. Srivani, D.; Gupta, A.; Bhosale, S.V.; Puyad, A.L.; Xiang, W.; Li, J.; Evans, R.A.; Bhosale, S.V. Non-fullerene acceptors based on central naphthalene diimide flanked by rhodamine or 1,3-indanedione. *Chem. Commun.* **2017**, *53*, 7080–7083. [[CrossRef](#)]
30. Hirade, M.; Yasuda, T.; Adachi, C. Effects of intramolecular donor–acceptor interactions on bimolecular recombination in small-molecule organic photovoltaic cells. *J. Phys. Chem. C* **2013**, *117*, 4986–4991. [[CrossRef](#)]
31. Sun, K.; Xiao, Z.; Lu, S.; Zajackowski, W.; Pisula, W.; Hanssen, E.; White, J.M.; Williamson, R.M.; Subbiah, J.; Ouyang, J.; et al. A molecular nematic liquid crystalline material for high-performance organic photovoltaics. *Nat. Commun.* **2015**, *6*, 6013. [[CrossRef](#)] [[PubMed](#)]
32. Gunawardhana, R.; Bulumulla, C.; Gamage, P.L.; Timmerman, A.J.; Udamulle, C.M.; Biewer, M.C.; Stefan, M.C. Thieno [3,2-b] pyrrole and Benzo [c] [1,2,5] thiadiazole donor-acceptor semiconductors for organic field-effect transistors. *ACS Omega* **2019**, *4*, 19676–19682. [[CrossRef](#)] [[PubMed](#)]
33. Gupta, V.; Lai, L.F.; Datt, R.; Chand, S.; Heeger, A.J.; Bazan, G.C.; Singh, S.P. Dithienogermole-based solution-processed molecular solar cells with efficiency over 9%. *Chem. Commun.* **2016**, *52*, 8596–8599. [[CrossRef](#)] [[PubMed](#)]
34. Gao, K.-J.; Li, L.; Lai, T.; Xiao, L.; Huang, Y.; Huang, F.; Peng, J.; Cao, Y.; Liu, F.; Russell, T.P.; et al. Deep absorbing porphyrin small molecule for high-performance organic solar cells with very low energy losses. *J. Am. Chem. Soc.* **2015**, *137*, 7282–7285. [[CrossRef](#)] [[PubMed](#)]
35. Abdullah; Akhtar, M.S.; Kim, E.-B.; Fijahi, L.; Shin, H.S.; Ameen, S. A symmetric benzoselenadiazole based D–A–D small molecule for solution processed bulk-heterojunction organic solar cells. *J. Ind. Eng. Chem.* **2020**, *81*, 309–316. [[CrossRef](#)]
36. Nazim, M.; Ameen, S.; Seo, H.-K.; Shin, H.S. Effective D-A-D type chromophore of fumaronitrile-core and terminal alkylated bithiophene for solution-processed small molecule organic solar cells. *Sci. Rep.* **2015**, *5*, 11143. [[CrossRef](#)]
37. Nazim, M.; Ameen, S.; Akhtar, M.S.; Shin, H.-S. Efficient spirobifluorene-core electron-donor material for application in solution-processed organic solar cells. *Chem. Phys. Lett.* **2016**, *663*, 137–144. [[CrossRef](#)]

38. An, B.-K.; Lee, D.-S.; Lee, J.-S.; Park, Y.-S.; Song, H.-S.; Park, S.Y. Strongly fluorescent organogel system comprising fibrillar self-assembly of a trifluoromethyl-based cyanostilbene derivative. *J. Am. Chem. Soc.* **2004**, *126*, 10232–10233. [[CrossRef](#)]
39. Tang, M.L.; Bao, Z. Halogenated materials as organic semiconductorst. *Chem. Mater.* **2011**, *23*, 446–455. [[CrossRef](#)]
40. Li, Z.; Wu, Z.; Fu, W.; Liu, P.; Jiao, B.; Wang, N.; Zhou, G.; Hou, X. Versatile fluorinated derivatives of triphenylamine as hole-transporters and blue-violet emitters in organic light-emitting devices. *J. Phys. Chem. C* **2012**, *116*, 20504–20512. [[CrossRef](#)]
41. Zitzler-Kunkel, A.; Lenze, M.R.; Kronenberg, N.M.; Krause, A.-M.; Stolte, M.; Meerholz, K.; Würthner, F. NIR-absorbing merocyanine dyes for BHJ solar cells. *Chem. Mater.* **2014**, *26*, 4856–4866. [[CrossRef](#)]
42. He, G.; Li, Z.; Wan, X.; Liu, Y.; Zhou, J.; Long, G.; Zhang, M.; Chen, Y. Efficient small molecule bulk heterojunction solar cells with high fill factors via introduction of p-stacking moieties as end group. *J. Mater. Chem. A* **2013**, *1*, 1801–1809. [[CrossRef](#)]
43. He, G.; Li, Z.; Wan, X.; Zhou, J.; Long, G.; Zhang, S.; Zhang, M.; Chen, Y. Impact of dye end groups on acceptor–donor–acceptor type molecules for solution-processed photovoltaic cells. *J. Mater. Chem.* **2012**, *22*, 9173. [[CrossRef](#)]
44. Qi, X.; Lo, Y.-C.; Zhao, Y.; Xuan, L.; Ting, H.-C.; Wong, K.; Rahaman, M.; Chen, Z.; Xiao, L.; Qu, B. Two novel small molecule donors and the applications in bulk-heterojunction solar cells. *Front. Chem.* **2018**, *6*, 260. [[CrossRef](#)] [[PubMed](#)]
45. Chen, X.; Feng, H.; Lin, Z.; Jiang, Z.; He, T.; Yin, S.; Wan, X.; Chen, Y.; Zhang, Q.; Qiu, H. Impact of end-capped groups on the properties of dithienosilole-based small molecules for solution-processed organic solar cells. *Dye. Pigment.* **2017**, *147*, 183–189. [[CrossRef](#)]



© 2020 by the authors. Licensee MDPI, Basel, Switzerland. This article is an open access article distributed under the terms and conditions of the Creative Commons Attribution (CC BY) license (<http://creativecommons.org/licenses/by/4.0/>).